Control of Coherent Acoustic Phonons in Semiconductor Quantum Wells

Ümit Özgür, Chang-Won Lee, and Henry O. Everitt*

Department of Physics, Duke University, Durham, North Carolina 27708
(Received 26 September 2000)

Using subpicosecond optical pump-probe techniques, coherent zone-folded longitudinal acoustic phonons (ZFLAPs) were investigated in an InGaN multiple quantum well structure. A two-pump differential transmission technique was used to generate and control coherent ZFLAP oscillations through the relative timing and amplitude of the two pump pulses. Enhancement and suppression of ZFLAP oscillations were demonstrated, including complete cancellation of generated acoustic phonons for the first time in any material system. Coherent control was used to demonstrate that ZFLAPs are generated differently in InGaN multiple quantum wells than in GaAs/AlAs superlattices.

The techniques of ultrafast optical spectroscopy have provided unprecedented capabilities to generate and control coherent quantum mechanical processes and to examine fundamental physical phenomena such as relaxation, dephasing, and squeezing. The ability to control coherent behavior is well established in atomic and molecular systems [1–3]. Control of coherent behavior in condensed matter systems has been more problematical [4], primarily because of the much faster dephasing times and difficulty of manipulating coherent states on time scales much shorter than this. Recent demonstrations of control and entanglement of excitonic and biexitonic states in semiconductor quantum dots [5] suggest that such problems are not insurmountable, and that control of coherent phenomena in condensed matter systems is achievable.

Inevitably, electron-phonon interactions limit the dephasing time of electronic or excitonic coherent states, so understanding and controlling the effects of phonons is of fundamental interest [6,7]. Particularly challenging is the optical investigation of acoustic phonons in bulk semiconductors because the phonon dispersion relation permits only low frequency Brillouin scattering. However, it is well understood that a semiconductor multiple quantum well (MQW) produces zone folding of the acoustic phonon branch so that direct excitation is possible [7–10]. Recently, it has been demonstrated that particularly strong coherent zone-folded longitudinal acoustic phonon (ZFLAP) oscillations can be generated and observed in InGaN MQW structures [11–13].

In this Letter, the optical mechanism for generating these coherent ZFLAP oscillations is shown to be impulsive, similar to the striking of a bell, much like the impulsive stimulated Raman Scattering (ISRS) technique [14]. Demonstration of coherent ZFLAP control follows, including the first complete cancellation of generated acoustic phonons in InGaN or any other material system. Coherent acoustic phonon control reveals that acoustic phonons are generated somewhat differently in InGaN MQWs than in GaAs/AlAs superlattices (SLs).

The MQW sample used here was grown by metal-organic chemical vapor deposition at the University of California at Santa Barbara using a modified two-flow horizontal reactor on double polished *c*-plane sapphire [15]. It consists of a ten period, 12 nm per period, MQW with 3.5 nm wide $In_{0.15}Ga_{0.85}N$ quantum wells and 8.5 nm wide $In_{0.05}Ga_{0.95}N$:Si barriers [16]. The MQW structure is capped with a 100 nm GaN layer and is grown on a ~ 2 μm GaN:Si layer. The Si doping concentration in the barriers is $\sim 10^{18}$ cm^{-3}.

In previous room temperature measurement of carrier capture in this sample, photoluminescence (PL) and photoluminescence excitation (PLE) spectroscopies identified the energies of the quantum well states and the barriers, respectively [13]. The peak PL emission occurred at 2.99 eV, corresponding to electron-hole recombination from the lowest energy quantum well subband states. The broad PLE absorption peak for emission at 2.99 eV occurred near 3.22 eV, corresponding to electron-hole (*e*-*h*) pairs being generated near the MQW barrier band edge.

Wavelength-degenerate, subpicosecond, pump-probe differential transmission (DT) has been used to measure the electron capture time [13]. A strongly wavelength-dependent biexponential decay of the created carriers (Fig. 1) indicated that electrons were captured with a time constant between 0.31–0.54 ps. Electrons were most efficiently captured from 3D barrier states to 2D confined QW states when *e*-*h* pairs were generated within 50 meV of the 3.22 eV barrier. Because of the greater density of states in the valence band, holes were captured too quickly to be measured. The strained material generates a large (~ 1 MV/cm) piezoelectric (PZE) field in the MQWs [17], and the width of the PL signal and region of efficient carrier capture (~ 100 meV) suggest sizable material inhomogenieties.

Remarkably strong damped oscillations in the DT signal are observed, suggesting the generation of coherent phenomena in the quantum wells (Fig. 1). The damped oscillations always started at the peak of the pump pulse ($t = 0$) and are described by $A \exp(-t/\tau) \cos(2\pi t/P + \pi)$, whose phase term π signifies that the oscillations were always observed to start at a minimum. Observing similar phenomena in similar MQW structures, Sun *et al.* [11,12]
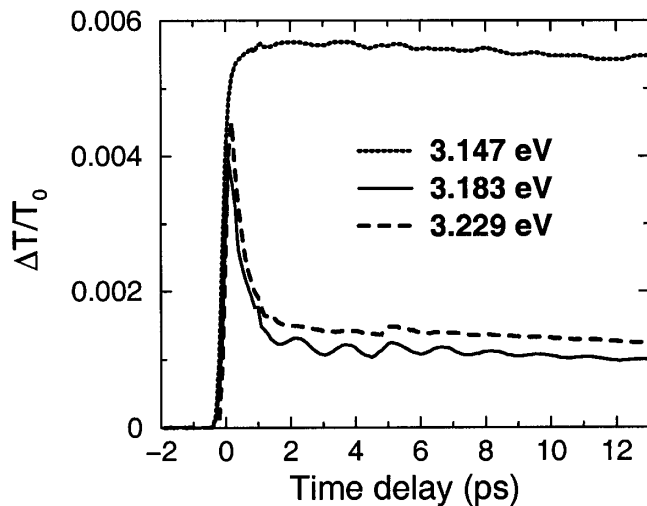
FIG. 1. Single pump DT data for pump/probe wavelengths near (3.229 and 3.183 eV) and below (3.147 eV) the barrier band edge. The feature at 5 ps arises from a pump pulse reflection from the substrate.
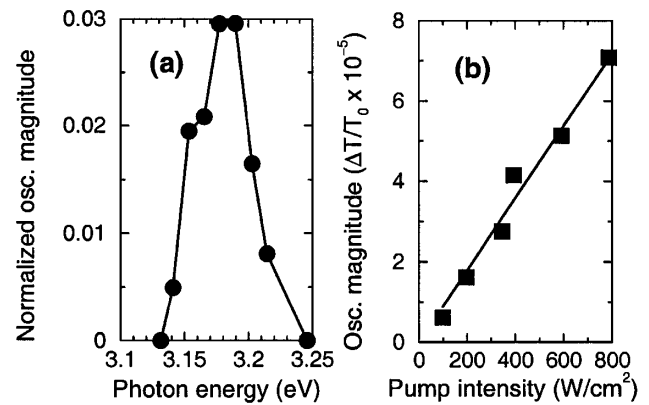

FIG. 2. (a) Strength of coherent ZFLAP oscillations as a function of pump/probe energy, normalized with respect to the peak $\Delta T/T_0$ value at that energy. (b) Strength of coherent ZFLAP oscillations as a function of pump intensity.

concluded that such oscillations are the manifestation of coherent ZFLAPs by demonstrating that the oscillation period P increased linearly with increasing MQW period d as $P = d/v_s$, where v_s is the sound velocity. The ZFLAPs propagate along the c axis of the wurtzitic InGaN. The oscillations observed in our $d = 12$ nm MQW sample occurred with a period $P = 1.44$ ps (frequency $= f_0 = 23$ cm^{-1}). Preliminary spontaneous Raman measurements confirmed a ZFLAP frequency of 23 cm^{-1}, yielding a sound velocity of 8333 m/s [18]. The measured characteristic damping time of these oscillations ($\tau = 12$ ps) sets a lower limit for the ZFLAP coherence time.

The sound velocity has not been measured directly in any InGaN material; however, the value in bulk GaN along the c axis is well established between 7990−8020 m/s [19,20]. Although InGaN is expected to be a softer material with a slower sound velocity, our low In content MQWs should not deviate much from the bulk GaN values. Using the c-axis elastic stiffness tensor element (C_{33}) and the density values for GaN (395 GPa, 6.087 g/cm^3) and InN (200 GPa, 6.890 g/cm^3) [21−23], the average sound velocity in the MQW region can be estimated to be 7888 m/s. The difference in the measured and calculated values may arise from the strain-induced piezoelectric field in the MQW region which tends to stiffen the material and raise the sound velocity along the c axis [19].

The coherent ZFLAP oscillations were strongest near the wavelength of most efficient carrier capture (3.18 eV) and were observed only within 40 meV of that energy [Fig. 2(a)]. Once carriers are captured into the wells, electrons and holes are separated by the strong PZE field and partially screen it. A nearly instantaneous change in the material stress results, impulsively inducing ZFLAP oscillations [14]. The screened PZE field also blueshifts the absorption band edge through the quantum-confined Franz-Keldysh effect (QCFKE). The ZFLAP oscillation modulates the carrier distribution that, in turn, modulates the strength of the QCFKE and the absorption band shift, thereby producing oscillations in the DT signal. Thus, the span of pump/probe energies over which ZFLAP oscillations are observed corresponds to the region of carrier capture and the width of the barrier absorption band edge.

To measure the dependence of the ZFLAP oscillation strength on pump intensity, the 3.183 eV pump and probe beams were focused to diameters of 75 and 40 μm, respectively. The time-averaged pump intensity was varied from 98 to 787 W/cm^2, while the probe intensity was kept at a constant 11 W/cm^2. Figure 2(b) demonstrates that the strength of the oscillations in this low excitation regime increases linearly with increasing pump intensity.

To achieve control of these coherent ZFLAPs, it is necessary to be able to manipulate them on time scales shorter than the oscillation period. The pulse widths of the frequency-doubled, 80 MHz Ti:sapphire laser pulses ($<$100 fs) and the temporal resolution (7 fs) of the 1 μm-per-step scanning motors of the delay lines for the DT pump-probe apparatus are much smaller than the ZFLAP oscillation period P. Coherent amplification and suppression of ZFLAPs may be demonstrated by the use of two-pump, one-probe DT. The relative timing of the two-pump pulses determines whether the coherent ZFLAP oscillations add constructively (e.g., delay $\Delta t = P$) or destructively (e.g., $\Delta t = P/2$). All three pulses were derived from the same frequency-doubled Ti:sapphire laser pulse and were independently delayed with respect to each other through the use of various beam splitters and delay stages. For simplicity, the pump pulses were delayed relative to a fixed length probe pulse pathway, and the two pump pulses were delayed relative to each other by the use of a second delay stage mounted on the first. The three beams were made to overlap on the sample by passing through a common lens in a coplanar geometry. The pump spot sizes were chosen to allow maximum pump intensity while ensuring the probe spot diameter was well within those of the two-pump spots.

Figure 3 demonstrates the coherent amplification ("in-phase", $\Delta t = P$) and cancellation ("out-of-phase," $\Delta t = P/2$) of room temperature ZFLAP oscillations. To examine the damped ZFLAP oscillations, a simple biexponential decay was fit to the data, beginning at the peak of the second pump curve. The residual of the fit reveals the damped oscillation of the ZFLAP, and a damped cosine oscillation was fit to the residual as before to measure the amplitude A_2 and decay τ_2 of the oscillation (Fig. 4). The simple, damped oscillation following the second pump suggests that the decay time of the second ZFLAP oscillation is the same as the first ($\tau_1 = \tau_2 = \tau$) and that phase coherence is maintained between the two oscillations for at least 12 ps.

Even though the first ZFLAP oscillations have decayed somewhat by the time of the second pump, it was observed that the intensity of the second pump must be *increased* relative to the first for exact amplitude doubling or cancellation. To provide a quantitative measure of the degree of amplification or suppression as a function of relative pump intensities, the amplitude A_2, referenced to the amplitude of the first ZFLAP oscillations at the time of the second pump $[A_1' = A_1 \exp(-\Delta t/\tau)]$, is plotted in Fig. 5 for both the in-phase and out-of-phase cases. Negative values for the out-of-phase A_2/A_1' indicate a relative π phase shift in amplitude, signifying that the second ZFLAP oscillations are stronger than the first. Roughly the same pump intensity is required to double the oscillations as to cancel them ($I_2/I_1 \approx 1.3$). Assuming the strength of the oscillations increases linearly with pump intensity [Fig. 2(b)], the predicted $A_2/A_1' = 1 \pm (I_2/I_1) \exp(\Delta t/\tau)$ roughly agrees with the data with no additional adjustable parameters for both in-phase ($+$) and out-of-phase ($-$) cases (Fig. 5). The slight discrepancy may be the result of PZE field screening by the carriers captured after the first pulse, reducing the efficiency of ZFLAP generation by the second pulse.
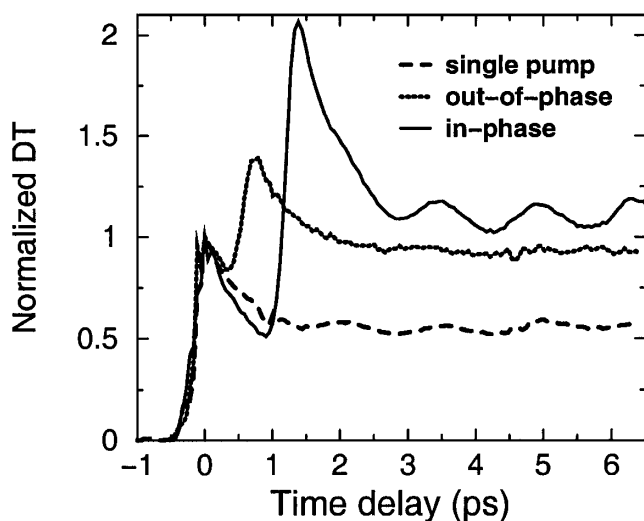
This ability to generate and control spectrally pure, very high frequency coherent ZFLAPs represents a new experimental regime for the phonon scientist. For the first time, a single acoustic phonon mode may be generated and controlled. Its spectral purity and strength derive from three attributes. First, in contrast with backscattering Raman, impulsive DT does not generate acoustic phonon doublets at frequencies determined by the wave vector of the incident light [24]. These phonon doublets are of great spectroscopic benefit but represent a tremendous hindrance for phonon control. Second, previous studies of ZFLAP oscillations in GaAs/AlAs SLs using forward-scattering ISRS revealed a fundamental ZFLAP mode ($f = f_0$) and its second harmonic ($f = 2f_0$) [7]. Two-pump phonon control was able to suppress the fundamental ZFLAP mode while enhancing its second harmonic, even when the second harmonic was not apparent in the one-pump data. By contrast, InGaN MQW ZFLAP overtone harmonics were surprisingly missing in the one- and two-pump configurations. As suggested by Fig. 4, the two-pump data most strongly supports the hypothesis of no overtones, and statistical analysis rejects overtones of any amplitude, relative to the fundamental, of more than 5%. Third, the one-pump, DT-induced ZFLAP oscillations were more than 10 times stronger than those reported for the GaAs/AlAs SL, even though the GaAs/AlAs SL had 4 times as many periods and was pumped almost 10 times harder [7]. The likely explanation again lies with the intrinsic strain-induced PZE field in the InGaN MQWs. Photogenerated carriers partially screen the PZE field, suddenly relieving some of the incredible strain in the MQWs and impulsively generating strong, coherent ZFLAP oscillations. The relative

FIG. 3. Time-resolved one-pump and two-pump DT data. The two pumps were one ZFLAP oscillation period apart (in-phase, $I_2/I_1 = 2.78$) or one-half ZFLAP oscillation period apart (out-of-phase, $I_2/I_2 = 1.31$).
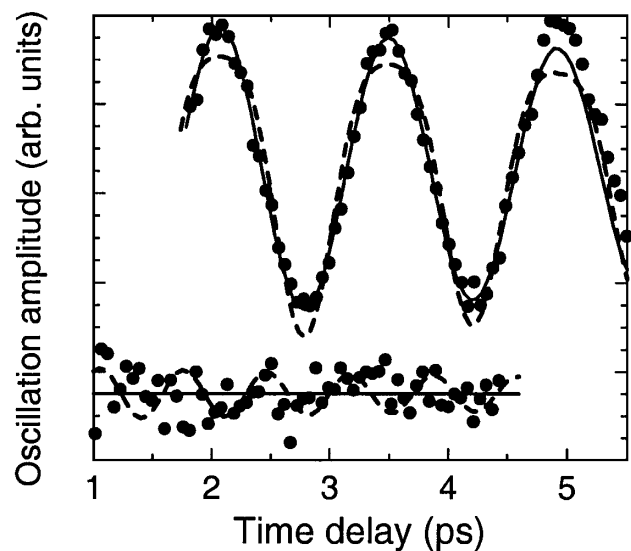

FIG. 4. The data residuals of the fits for biexponential decay reveal the damped coherent ZFLAP oscillations for both two-pump cases in Fig. 3. The solid line represents the best fit assuming no overtone harmonics, and the dashed line illustrates the inferiority of the best fit including a second harmonic 20% as strong as the first.
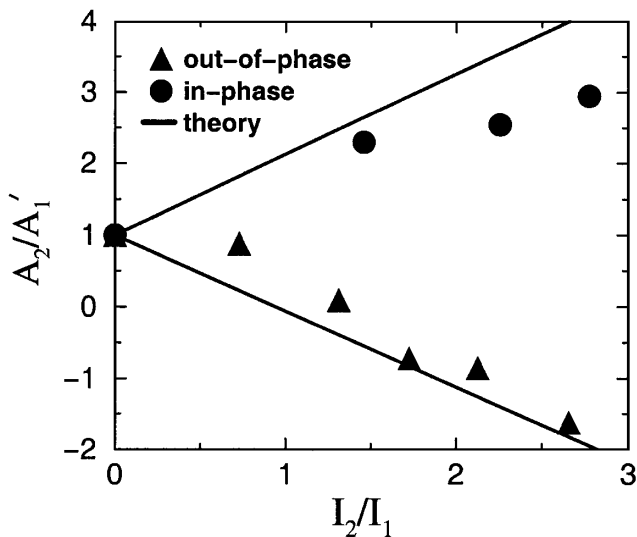
FIG. 5.   Strengths of the ZFLAP oscillations induced by the second pump, relative to those induced by the first pump, as a function of the ratio of the two-pump intensities.

strain relief is apparently much greater than the strain induced by the ISRS photogenerated carriers in unstrained GaAs/AlAs SLs.

The out-of-phase data in Fig. 3 represent the first experimental demonstration of complete coherent acoustic phonon cancellation in any material system. The scientific and technological utility of single mode acoustic phonon generation and control is made even more attractive by the fact that it requires merely a standard 80 MHz, unamplified, mode-locked Ti:sapphire laser, two delay stages, and a room temperature, short period MQW. Already, coherent control of ZFLAPs has revealed a fundamental difference in the generation of acoustic phonons in GaAs/AlAs SLs and InGaN MQWs. In addition, it is now possible to cancel coherent ZFLAPs one-half period after their creation. The resulting single mode acoustic phonon impulse can propagate through the sample and may be traced temporally or mapped spatially. Conversely, repeated excitation with multiple in-phase pulses can continue to amplify the ZFLAP oscillations parametrically, permitting an investigation of phonon "gain," acoustic nonlinearity, and the role of the PZE field. These coherent techniques will enable unprecedented investigations of poorly understood acoustic phonon reflection and transmission at interfaces, with substrates, or in other materials to which the MQW is bonded. More generally, complex temporal pump pulse waveforms, created by genetic learning algorithms [25] and spatial light modulators [26], can be used as a coherent terahertz ultrasonic transducer to create nontrivial phonon excitations to explore or control phonon mediated decay or dephasing of carriers and excitons.

The samples were grown by A. C. Abare, S. Keller, and S. P. DenBaars of the University of California, Santa Barbara. We thank R. Merlin for numerous valuable dis-

*Also at U.S. Army Research Office, Research Triangle Park, Durham, North Carolina 27709-2211.
  Electronic address: everitt@arl.aro.army.mil
[1] W. S. Warren, H. Rabitz, and M. Dahleh, Science **259**, 1581 (1993).
[2] Z. D. Gaeta, M. Noel, and C. R. Stroud, Jr., Phys. Rev. Lett. **73**, 636 (1994).
[3] T. C. Weinacht, J. Ahn, and P. H. Bucksbaum, Nature (London) **397**, 233 (1999).
[4] P. Gross et al., Phys. Rev. B **49**, 11 100 (1994).
[5] N. H. Bonadeo et al., Science **282**, 1473 (1998).
[6] K. Schwab, E. A. Henriksen, J. M. Worlock, and M. L. Roukes, Nature (London) **404**, 974 (2000).
[7] A. Bartels, T. Dekorsy, H. Kurz, and K. Köhler, Appl. Phys. Lett. **72**, 2844 (1998).
[8] C. Colvard et al., Phys. Rev. B **31**, 2080 (1985).
[9] A. V. Kuznetsov and C. J. Stanton, Phys. Rev. Lett. **73**, 3243 (1994).
[10] K. Mizoguchi, M. Hase, S. Nakashima, and M. Nakayama, Phys. Rev. B **60**, 8262 (1999).
[11] C. K. Sun et al., Appl. Phys. Lett. **75**, 1249 (1999).
[12] C. K. Sun, J. C. Liang, and X. Y. Yu, Phys. Rev. Lett. **84**, 179 (2000).
[13] Ü. Özgür et al., Appl. Phys. Lett. **77**, 109 (2000).
[14] R. Merlin, Solid State Commun. **102**, 207 (1997).
[15] S. Keller et al., J. Cryst. Growth **195**, 258 (1998).
[16] X-ray measurements of the sample revealed the MQW period to be 12 nm, not the 8 nm originally claimed by the growers and reported in [13].
[17] T. Takeuchi et al., Appl. Phys. Lett. **73**, 1691 (1998).
[18] This value is significantly larger than the 6800 m/s reported in [11,12], although the samples used in this study and in [11,12] were nearly identical and grown by the same laboratory. Indeed, our results concurred with [11,12] until we discovered the error in the reported MQW period [16] which accounts for the discrepancy.
[19] C. Deger et al., Appl. Phys. Lett. **72**, 2400 (1998).
[20] M. Yamaguchi et al., J. Appl. Phys. **85**, 8502 (1999).
[21] K. Kim, W. R. L. Lambrecht, and B. Segall, Phys. Rev. B **53**, 16 310 (1996).
[22] A. F. Wright, J. Appl. Phys. **82**, 2833 (1997).
[23] H. Morkoç, *Nitride Semiconductors and Devices* (Springer-Verlag, Berlin, 1999).
[24] A. Bartels, T. Dekorsy, H. Kurz, and K. Köhler, Phys. Rev. Lett. **82**, 1044 (1999).
[25] F. G. Omenetto, B. P. Luce, and A. J. Taylor, J. Opt. Soc. Am. B **16**, 2005 (1999).
[26] A. M. Weiner, Rev. Sci. Instrum. **71**, 1929 (2000).